

Ultrafast photodimerization dynamics in α -cyano-4-hydroxycinnamic and sinapinic acid crystals

Theo Hoyer *, Wilfried Tuszynski, Christoph Lienau

Institut für Physik, Carl von Ossietzky Universität, D-26111 Oldenburg, Germany

Received 26 February 2007; in final form 3 May 2007

Available online 13 June 2007

Abstract

We report a sub-picosecond time-resolved fluorescence spectroscopic study of different cinnamic acid crystals, model systems for solid-state photodimerization reactions. For α -cyano-4-hydroxycinnamic acid (α -CHC), we identify the emission spectra of both monomers and dimers, allowing us to directly probe the photoinduced dynamics of both species. The dimerization occurs on a timescale of 10 ps and results in a long-lived dimer product, stable for hours. For sinapinic acid, we find an extremely fast, sub-picosecond dimerization reaction and a short-lived dimer. This first sub-picosecond time-resolved dimerization study in cinnamic acid crystals provides a new basis for relating their structural properties and microscopic reaction dynamics.

© 2007 Elsevier B.V. All rights reserved.

1. Introduction

Since many years, crystals of cinnamic acid and its derivatives are important model systems for photoinduced chemical reactions in the solid state [1]. When illuminated with ultraviolet light, many of these substances undergo a configurational transformation of the crystalline lattice structure, either by photodimerization or photopolymerization [2–4]. These classical photoinduced solid-state phase changes originating from the parallel stacking of cinnamic acids have been the subject of numerous investigations, employing a variety of different experimental techniques, including X-ray structural analysis [5], NMR [5], UV absorption [6], infrared [7,8] and Raman spectroscopy [9] and atomic force microscopy [10].

Despite this continuing interest, very little is known about the microscopic dynamics of these photoinduced phase transformations. This is all the more surprising as cinnamic acids are not only interesting from a basic science point of view but find various applications as UV absorbers

in sun creams [11] or liquid crystal displays [12], and show antioxidant [13] and antibacterial activity [14]. Also, the derivatives α -cyano-4-hydroxycinnamic acid (α -CHC) and 3,5-dimethoxy-4-hydroxycinnamic acid (sinapinic acid, SA) are important and well established matrix substances in matrix-assisted laser desorption/ionization mass spectrometry (MALDI-MS) [15–18]. Therefore elucidating the photodimerization dynamics in cinnamic acids may prove particularly useful in unravelling some of the not yet fully understood elementary ablation and ionization processes in MALDI applications.

In liquid solution, the ultrafast dynamics of cinnamic acid derivatives have recently been carefully studied by using broad-band femtosecond (fs) pump-probe spectroscopy [19]. Excitation with UV light results in an ultrafast photoisomerization occurring on a time scale of few picoseconds (ps), followed by vibrational cooling in the ground state. Here, in the absence of crystalline order, the photodimerization channel is not available. Analysis of the solid-state photodimerization dynamics of cinnamic acid derivatives has been attempted by means of a ps time-resolved X-ray diffraction study [20]. So far, however, these experiments could not yet reveal an unambiguous signature of the photoinduced dimerization dynamics.

* Corresponding author. Fax: +49 441 798 3890.

E-mail address: theo.hoyer@uni-oldenburg.de (T. Hoyer).

In this Letter, we report the first direct experimental study of the photodimerization dynamics in cinnamic acids. Using quasi-stationary photoluminescence (PL) spectroscopy, we identify the emission signatures of both α -CHC monomers and dimers. This allows us to follow the time evolution of the photoinduced monomer and dimer populations by means of fs- and ps-time-resolved photoluminescence spectroscopy, providing a direct measurement of the dimerization dynamics. For α -CHC, the dimerization occurs on a time scale of few tens of ps, and results in a dimer molecule which is stable for at least hours. For sinapinic acid, on the other hand, we find an extremely fast, sub-picosecond dimerization reaction and a short-lived dimer product, decaying on a μ s time scale, is formed. We tentatively attribute these drastic changes of the reaction dynamics to the different crystalline structures of these substances.

2. Experimental

The cinnamic acids α -CHC and SA were used as purchased from Fluka without further purification or after recrystallisation in ethanol. For steady-state and ps time-resolved PL measurements, a small amount (5–10 mg) of the substance was deposited on a quartz substrate and dissolved in a droplet of ethanol. This results in a microcrystalline sample layer with a thickness of about 1 μ m. Typical dimensions of the microcrystallites are about 20–50 μ m. The samples for the fluorescence up-conversion studies were prepared by spray deposition using a nebulizer. 0.25 ml of a solution of 10 mg α -CHC or SA dissolved in 1 ml of ethanol was spray-deposited onto a rotating quartz slide via a nitrogen stream. This method results in a spatially homogeneous, microcrystalline, 1-cm-large sample layer with an average thickness of about 15 μ m.

For steady-state and ps PL measurements we used a synchronously pumped, cavity-dumped dye laser system. When using DCM as a laser dye, this system produced 15 ps light pulses at a wavelength of 660 nm and a repetition rate of 4 MHz. The excitation pulses at 330 nm were created by second-harmonic generation in a LiNbO₃ crystal and were focused onto the sample to a spot size of 100 μ m. Typical pulse energies were about 100 pJ. The sample fluorescence was collected in reflection in a confocal geometry. For recording steady-state PL spectra, the fluorescence was dispersed in a 0.5 m monochromator and detected with a liquid-nitrogen-cooled, back-illuminated charge-coupled device (CCD). For the ps time-resolved measurements, the fluorescence was passed through a subtractive, 0.25 m double monochromator and detected by a micro-channel plate photomultiplier tube (MCP-PMT, Hamamatsu R3809U-50). Using a home-built time-correlated single photon counting (TCSPC) electronics, we achieve in this setup a width of the response function of 50 ps (full-width-at-half-maximum, FWHM).

For PL measurements with femtosecond time resolution, we used a fluorescence up-conversion setup as

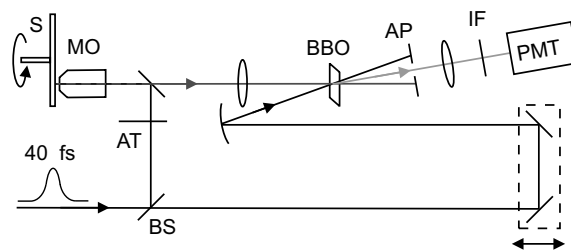


Fig. 1. Schematic of the fluorescence up-conversion setup. 40 fs pulses from a Ti:Sapphire oscillator operating at 800 nm are focused at a pulse energy of 1 nJ through a microscope objective (MO) to a 3 μ m spot size onto the rotating sample (S). The two-photon-induced fluorescence is collected and time-gated in a BBO crystal. The up-converted signal is detected using a cooled PMT.

depicted schematically in Fig. 1. A Ti:Sapphire system was used to generate 40 fs laser pulses at a center wavelength of $\lambda_L = 800$ nm and a repetition rate of 80 MHz. The excitation pulses were split off at a beam splitter (BS) and attenuated with a normal density filter (AT) to a pulse energy of about 1 nJ. These pulses were focused to a spot size of about 3 μ m onto the sample using a microscope objective (MO) with a numerical aperture of 0.35. To avoid excitation-induced bleaching effects, the sample was mounted on a rotation stage (S), rotating at about 20 Hz, and the focal spot was off-set by 3 mm from the rotation axis. Two-photon-induced fluorescence from the sample was collected via the same microscope objective, focused into a 3-mm-thick beta-barium-borate (BBO) crystal and mixed with the time-delayed gate pulses from the Ti:Sapphire laser. To probe the time-gated two-photon-induced sample fluorescence at wavelength λ_F , the up-converted signal at the sum frequency $c(\lambda_L^{-1} + \lambda_F^{-1})$ was spectrally filtered out using an interference filter (IF) with a bandwidth of 5 nm and detected by a cooled PMT. To reduce background noise, the PMT pulses were electronically gated using the TCSPC electronics. This setup allows us to probe fluorescence with a time resolution of 250–300 fs as independently verified by recording the time structure of the second-harmonic radiation at a wavelength of 400 nm generated in 3-hydroxypicolinic acid layer [inset in Fig. 4b]. The time resolution is mainly limited by the dispersion of the microscope objective. Two-photon excitation was mainly used to optimize both spatial and temporal resolution of the experiment. The high spatial resolution of our setup of 3 μ m allows us to insure that possible sample inhomogeneities do not affect the fluorescence dynamics.

3. Results

The fluorescence spectrum of a freshly prepared microcrystalline α -CHC layer [Fig. 2a, 0 s] shows a sharp onset at 440 nm, different vibronic replicas and a tail extending to about 650 nm. When illuminated with 330 nm picosecond pulses at an average intensity of 5 W/cm², the PL spectrum transforms gradually with increasing illumination

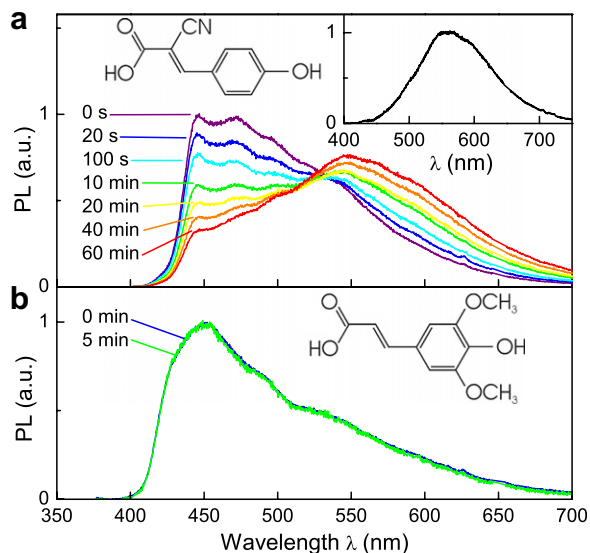


Fig. 2. (a) Fluorescence spectra of α -CHC recorded for 330 nm excitation at an intensity of 5 W/cm^2 . The featureless emission band at around 550 nm, growing in intensity with increasing irradiation time, is assigned to the emission from α -CHC dimers. Inset: Emission spectrum of α -CHC dimers and (b) fluorescence spectra of microcrystalline SA, recorded under identical excitation conditions. No signatures for photodimerization are observed.

time, showing a continuous decrease of the α -CHC monomer emission and a concomitant rise of a new, spectrally broad and featureless emission band, centered around 550 nm. We assign this new band to the emission from α -CHC dimers, formed by photodimerization. Subtracting the appropriately normalized α -CHC monomer emission spectrum from the emission at finite illumination times allows us to isolate the emission spectrum of α -CHC dimers [Fig. 2a, inset]. For α -CHC, the photoinduced modifications of the emission persist for at least several hours after stopping the illumination. It is also important to note that we do not observe modifications of the emission spectra when decreasing the illumination intensity by two orders of magnitude. This indicates that, under our excitation conditions, the relative strength of the monomer and dimer emission depends on the total laser fluence, but not on the momentary laser intensity.

For freshly prepared, microcrystalline sinapinic acid, the fluorescence spectrum [Fig. 2b] is qualitatively similar to that of α -CHC. Here, however, we do not observe a photo-induced modification of the fluorescence spectrum with increasing illumination time. This is evidently a signature that stable dimers are not formed in this material, or, to be more precise, that the quasi-stationary photoinduced dimer concentration is too low to be detected with our experimental apparatus. This absence of photodimerization has consistently been observed in various microcrystalline SA samples.

We now turn to time-resolved PL measurements on these samples. Fluorescence decay traces of α -CHC and SA for various detection wavelengths λ_d , recorded using

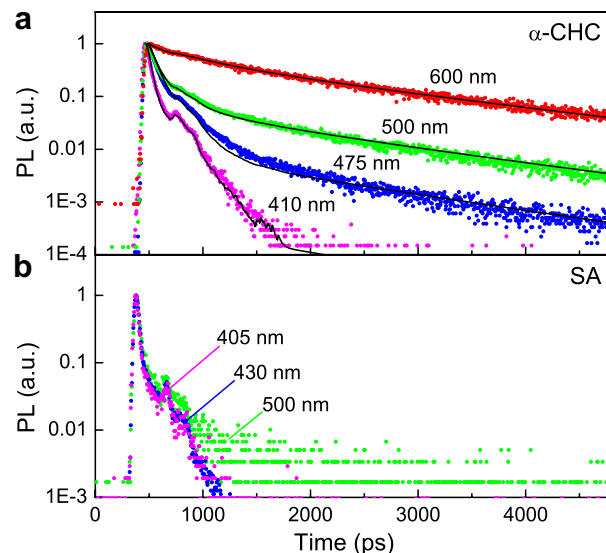


Fig. 3. Fluorescence decay curves for α -CHC (a) and SA (b) at different detection wavelengths λ_d (circles). All curves are recorded using TCSPC for excitation with 15 ps laser pulses at 330 nm and are plotted on a logarithmic intensity scale after normalization. The solid lines show a modelling of the decay dynamics within the phenomenological dimerization model introduced in the text. The decay curve for SA at $\lambda_d = 405 \text{ nm}$ reflects the instrumental response function of the setup.

TCSPC after excitation at 330 nm, are shown in Fig. 3a and b, respectively. For detection in the blue, $\lambda_d = 410 \text{ nm}$, we find a fast exponential decay with a lifetime of about $35 \pm 15 \text{ ps}$, just slightly beyond the time resolution of this experiment. When increasing λ_d to the red, we observe, in addition to the fast initial decay, a second, long-lived and non-exponential decay. The amplitude of this long-lived component increases with increasing λ_d and fully dominates the PL decay at $\lambda_d = 600 \text{ nm}$, where the fast initial decay is no longer discernible. For SA, the decay curves are essentially identical to the instrument response function. Obviously here, the PL decay time is much faster than the time resolution. Only at long wavelengths, $\lambda_d = 500 \text{ nm}$, a very faint long-lived component appears. The amplitude of this long-lived component reduces even further when decreasing the laser repetition rate to 40 kHz.

To get more insight into these fast luminescence processes, we increased the time-resolution of our setup by using a fluorescence-up-conversion technique and two-photon femtosecond excitation at 800 nm [Fig. 4]. In these experiments, the time resolution of 250 fs is sufficient to resolve the fast initial PL decay at $\lambda_d = 430 \text{ nm}$ in both α -CHC and SA. For α -CHC [Fig. 4a] we find a non-exponential decay on a 20-ps-timescale. For SA [Fig. 4b] the PL decay is much faster, as anticipated from the TCSPC measurements. The PL lifetime is $400 \pm 100 \text{ fs}$.

4. Discussion

We now discuss these results, presenting the first experimental study of the ultrafast photodimerization dynamics

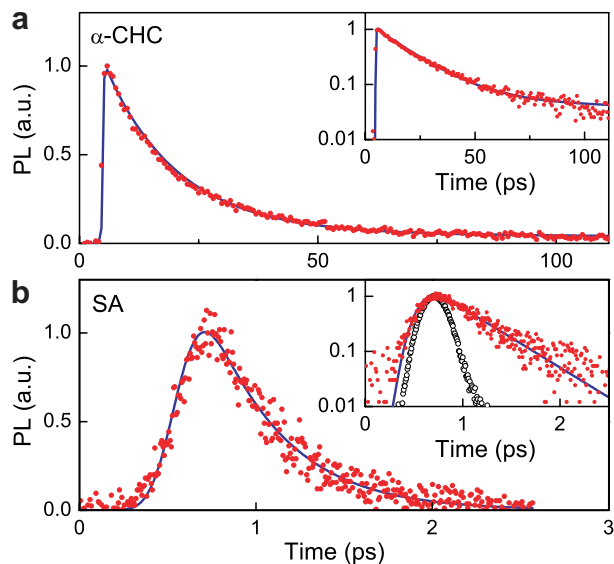


Fig. 4. Normalized fluorescence decay curves of crystalline α -CHC (a) and SA (b) recorded using fluorescence up-conversion. The data are taken at $\lambda_d = 430$ nm after two-photon excitation at 800 nm. The solid lines represent fits to the dimerization model. In the insets, the data are shown on a logarithmic intensity scale, together with the instrument response function (open circles).

in cinnamic acid crystals. In principle, all the ps and fs dynamics reported in Figs. 3 and 4 may be assigned to fast intramolecular relaxation and recombination dynamics within the α -CHC and SA monomers. Yet, the initial decay on a 10-ps-timescale found for α -CHC at blue detection wavelengths appears too slow to reflect the intramolecular vibrational relaxation dynamics within these molecules [19]. Also, and more importantly, such a unimolecular model does not account for the irradiation-induced generation of a new and pronounced emission band around 550 nm.

We therefore propose a different relaxation scenario [Fig. 5] involving the photodimerization dynamics. We essentially assume that the fast decay dynamics in both α -CHC and SA reflects the photodimerization process.

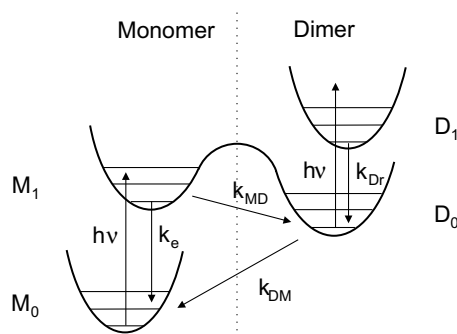


Fig. 5. Schematic of the molecular states and reaction dynamics involved in the phenomenological photo-induced dimerization model for cinnamic acids introduced in the text.

This means that the decay of the photoexcited monomer population

$$d[M_1(t)]/dt = -(k_{MD} + k_e)[M_1(t)] = -k_M[M_1(t)] \quad (1)$$

is dominated by a dimerization rate k_{MD} , rather than by radiative recombination and other unimolecular decay processes such as internal conversion (IC) represented by a total decay rate k_e . The data in Fig. 4b suggest that in SA this dimerization occurs on a sub-ps-timescale, $k_{MD}(\text{SA}) = (0.4 \text{ ps})^{-1}$. In α -CHC, the dimerization dynamics is apparently much slower, $k_{MD}(\alpha\text{-CHC}) = (20 \text{ ps})^{-1}$. The finding that the fast initial decay due to dimerization contributes less to the decay curves for α -CHC in the red spectral range reflects the gradual decrease of the α -CHC monomer fluorescence [Fig. 2a].

Upon photodimerization, the dimers can be formed either in their electronic ground (D_0) or excited state (D_1). Excited D_1 state dimers would give rise to pronounced dimer fluorescence. This is neither observed for freshly prepared α -CHC samples [Fig. 2a, 0 s] nor for SA. We therefore conclude that the dimerization reaction proceeds to the ground state D_0 .

Dimer fluorescence can be induced by sequential two-photon absorption ($M_0 \rightarrow M_1, D_0 \rightarrow D_1$) within the duration of the excitation pulses. Under our conditions, however, the probability for exciting an individual molecule is small (typically 10^{-4} within the first 50 nm) and a two-photon-induced dimer fluorescence can be ruled out. Such a two-photon dimer fluorescence would give rise to strongly intensity-dependent fluorescence spectra, in contrast to the intensity independence of our experimental data in Fig. 2.

If the lifetime k_{DM}^{-1} of the cinnamic acid dimers is longer than the time interval between two consecutive excitation pulses (0.25 μs for the ps and 13 ns for the fs experiments), the continuous illumination of the sample will give rise to the build-up of a quasi-stationary dimer concentration $\langle[D_0]\rangle$ which is much larger than the dimer concentration created with each individual pulse. For α -CHC this condition is certainly fulfilled as the experiments shown in Fig. 2a indicate a lifetime k_{DM}^{-1} of at least several hours. Therefore two different processes can be induced by the excitation pulses. Either the $M_0 \rightarrow M_1$ monomer transition is excited, giving rise to the short-lived fluorescence decay in the blue spectral region in Figs. 3 and 4, or the $D_0 \rightarrow D_1$ dimer transition can be excited. The induced dimer fluorescence $D_1 \rightarrow D_0$ is the origin of the long-lived fluorescence decay observed at wavelengths between 475 and 600 nm in Fig. 3a. Obviously, these long-lived fluorescence dynamics are not well described by monoexponential decays, indicating that the decay of the excited dimer D_1 population does not just originate from radiative recombination with rate k_{Dr} . We find that we can satisfactorily describe the experimental decay curves by assuming that an isotropic diffusion-limited bimolecular recombination process contributes significantly to the dimer decay

$$\frac{d[D_1(t)]}{dt} = -k_{Dr}[D_1(t)] - 2\frac{\beta}{[D_{1,0}]\sqrt{t}}[D_1(t)]^2. \quad (2)$$

Here, $[D_{1,0}] = [D_1(t=0)]$ is the maximum photoinduced dimer concentration (about $(20 \text{ nm})^{-3}$ in the ps experiments). For δ -pulse excitation, Eq. 2 gives

$$[D_1(t)] = [D_{1,0}] \cdot \frac{\exp(-k_{Dr}t)}{2\beta\sqrt{\pi/k_{Dr}} \cdot \text{erf}(\sqrt{k_{Dr}t}) + 1}. \quad (3)$$

Convolution with the instrument response function then gives the fluorescence decay dynamics. Such a bimolecular recombination dynamics is well known for polymer nanostructures [21–23], where exciton–exciton annihilation plays an important role. This model assumes randomly distributed, spatially fixed dimers in the microcrystals, and also an initially spatially random distribution of the optical excitations of these dimers. We assume that the dimers remain spatially fixed but that the optical excitations can diffuse within the dimer moiety, e.g., induced by near-field coupling, i.e., a Foerster type of energy transfer. This slow diffusive transport of dimer excitons is described by a diffusion constant D and exciton–exciton annihilation occurs whenever two excitations reach a certain critical contact distance R_0 , typically given by the exciton Bohr radius, i.e., in our case approximately the lattice constant. Then, the recombination parameter β is given as $\beta = 4R_0^2[D_{1,0}]\sqrt{\pi D}$.

For α -CHC we find good qualitative agreement between the experimental results obtained with both the TCSPC and fluorescence up-conversion setups and the predictions from this phenomenological dimerization model if we assume, in addition to the dimerization rate k_{MD} , a radiative dimer recombination rate $k_{Dr} = (1.8 \text{ ns})^{-1}$ and an annihilation parameter $\beta = 0.03 \text{ ps}^{-1/2}$. Due to the different excitation conditions and the reduced photoinduced dimer concentration $[D_{1,0}]$, the annihilation parameter in the up-conversion experiments is larger, about $\beta = 0.14 \text{ ps}^{-1/2}$. These annihilation parameters correspond to diffusion coefficients of the order of $0.1 \text{ cm}^2/\text{s}$, a typical value for conjugated polymers [23]. For obtaining a full quantitative agreement between the data of the TCSPC experiments and the dimerization model, we have to allow for a slight wavelength dependence of the dimerization rate (varying from $[35 \text{ ps}]^{-1}$ at 410 nm to $[55 \text{ ps}]^{-1}$ at 500 nm) and the dimer recombination rate k_{Dr} (varying from $[1.5 \text{ ns}]^{-1}$ at 475 nm to $[1.8 \text{ ns}]^{-1}$ at 600 nm). Decay curves calculated with optimized fit parameters are shown in Figs. 3 and 4, respectively. We believe that these parameter variations mainly stem from a not yet fully quantitative and oversimplified description of the annihilation dynamics. Such a phenomenological exciton–exciton annihilation model in the weak diffusion limit describes the non-exponential decay of the α -CHC dimer fluorescence satisfactorily. At present, we can, however, not rule out that other mechanisms contribute to this non-exponential decay. In particular, one may assume that fluctuations of the dimer structure and/or surrounding result in an inhomogeneous

distribution of dimer decay rates. Certainly, more work is needed to fully evidence the predicted diffusion transport of dimer excitons.

This phenomenological dimerization model also accounts for the photoinduced fluorescence dynamics in sinapinic acid. Here, however, the dimer lifetime k_{DM}^{-1} is orders of magnitude faster than in α -CHC. From the TCSPC experiments with variable repetition rates, we roughly estimate a lifetime of about $k_{DM}^{-1} \simeq 100 \text{ } \mu\text{s}$. This means that the quasi-stationary dimer concentration $\langle[D_0]\rangle$ in SA is much less than that in α -CHC and therefore the dimer fluorescence is strongly reduced. Basically, the dimer fluorescence is only apparent in the fluorescence decay curves at $\lambda_d = 500 \text{ nm}$, indicating a lifetime of the dimer excited state of 1–2 ns. This long-lived fluorescent component rules out that the PL decay of SA is solely described by a fast unimolecular decay process such as IC.

In summary, we have presented a first spectrally and temporally resolved fluorescence spectroscopic study of the photoinduced dimerization dynamics in cinnamic acid crystals. Based on an identification of the emission spectrum of α -CHC dimers, we were able to temporally resolve the dimerization dynamics. These dynamics depend apparently very sensitively on the geometric configurations of those crystals. For α -CHC, the dimerization occurs on a time scale of 10 ps and results in the formation of a dimer product which is stable for hours. In sinapinic acid, the photoexcited monomer lives only for about 0.5 ps and also the dimer product is only short-lived. These dramatic changes have obviously their origin in the different molecular structures, probably in the type and number of substituents at the phenyl ring, and in the case of SA one may speculate that in the crystalline phase the strict alignment of the molecules and the network of hydrogen bondings within the [103] plane [24] plays a decisive role in its reaction dynamics. In any case we anticipate that the new results presented in this work will stimulate more detailed investigations of the interplay between microscopic reaction dynamics and crystallographic configurations in cinnamic acids, and, more generally, other prototypical solid-state phase transitions. Newly emerging experimental tools such as ultrafast X-ray and electron diffraction, and also ultrafast infrared spectroscopy, may be of paramount importance for such investigations. Also, one may hope that the new information on the photophysics of cinnamic acids given here may prove useful in elucidating some of the elementary processes in MALDI applications.

Acknowledgements

We thank Stefan Bleil for his help in building up the fluorescence up-conversion experiment, Dirk Otteken for expert technical assistance and Karlheinz Maier for continuous support.

References

- [1] M.D. Cohen, G.M.J. Schmidt, F.I. Sonntag, *J. Chem. Soc.* (1964) 2000.
- [2] M. Hasegawa, *Chem. Rev.* 83 (1983) 507.
- [3] K. Tanaka, F. Toda, *Chem. Rev.* 100 (2000) 1025.
- [4] T. Frišćić, L.R. MacGillivray, *Z. Kristallogr.* 220 (2005) 351.
- [5] V. Enkelmann, G. Wegner, *J. Am. Chem. Soc.* 115 (1993) 10390.
- [6] J. Davaasambu, G. Busse, S. Techert, *J. Phys. Chem. A* 110 (2006) 3261.
- [7] S.D.M. Atkinson et al., *J. Chem. Soc. Perkin Trans. 2* (2002) 1533.
- [8] S.D.M. Atkinson, M.J. Almond, S.J. Hibble, P. Hollins, S.L. Jenkins, M.J. Tobin, K.S. Wiltshire, *Phys. Chem. Chem. Phys.* 6 (2004) 4.
- [9] M. Gosh, S. Chakrabarti, T.N. Misra, *J. Raman Spectrosc.* 29 (1998) 263.
- [10] G. Kaupp, *Angew. Chem. Int. Ed. Engl.* 31 (1992) 31.
- [11] R. Roelandts, *Clin. Exp. Dermatol.* 23 (1998) 147.
- [12] J. Hoogboom, T. Rasing, A.E. Rowan, R.J.M. Nolte, *J. Mater. Chem.* 16 (2006) 1305.
- [13] F. Natella, M. Nardini, M. Di Felice, C. Scaccini, *J. Agric. Food Chem.* 47 (1999) 1453.
- [14] J. Zhu, M. Majikina, S. Tawata, *Biosci. Biotechnol. Biochem.* 65 (2001) 161.
- [15] M. Karas, F. Hillenkamp, *Anal. Chem.* 60 (1988) 2299.
- [16] R.C. Beavis, B.T. Chait, *Proc. Nat. Acad. Sci.* 87 (1990) 6873.
- [17] R.C. Beavis, T. Chaudhary, B.T. Chait, *Org. Mass Spectrom.* 27 (1992) 156.
- [18] R. Zenobi, R. Knochenmuss, *Chem. Rev.* 103 (2003) 441.
- [19] J.L.P. Lustres, V.M. Farztdinov, S.A. Kovalenko, *Chem. Phys. Chem.* 6 (2005) 1590.
- [20] G. Busse, T. Tschentscher, A. Plech, M. Wulff, B. Frederichs, S. Techert, *Faraday Discuss.* 122 (2002) 105.
- [21] T.-Q. Nguyen, I.B. Martin, J. Liu, B.J. Schwartz, *J. Phys. Chem. B* 104 (2000) 237.
- [22] A. Dogariu, D. Vacar, A.J. Heeger, *Phys. Rev. B* 58 (1998) 10218.
- [23] E.S. Maniloff, V.I. Klimov, D.W. McBranch, *Phys. Rev. B* 56 (1997) 1876.
- [24] R.C. Beavis, J.N. Bridson, *J. Phys. D: Appl. Phys.* 26 (1993) 442.